

## Influence of university campus spatial morphology on outdoor thermal environment: A case study from Eastern China

Yansu Qi<sup>a,b,c</sup>, Lan Chen<sup>c</sup>, Jiuzhe Xu<sup>d</sup>, Chao Liu<sup>c</sup>, Weijun Gao<sup>a,b,c</sup>, Sheng Miao<sup>b,d,\*</sup>

<sup>a</sup> Innovation Institute for Sustainable Maritime Architecture Research and Technology, Qingdao University of Technology, Qingdao 266033, China

<sup>b</sup> Faculty of Environmental Engineering, The University of Kitakyushu, Kitakyushu 808-0135, Japan

<sup>c</sup> School of Environmental and Municipal Engineering, Qingdao University of Technology, Qingdao 266033, China

<sup>d</sup> School of Information and Control Engineering, Qingdao University of Technology, Qingdao 266033, China

### ARTICLE INFO

#### Keywords:

Spatial morphology  
Unmanned aerial vehicles  
Outdoor thermal comfort  
ENVI-met

### ABSTRACT

Outdoor thermal comfort is crucial for creating sustainable and livable urban spaces. Studying the distribution and impact factors of the thermal environment can provide theoretical support for improving the thermal environment and spatial planning. This study investigates the influence of well-defined boundary spaces on outdoor thermal comfort and proposes design measures to improve spatial thermal comfort. High-resolution data obtained from unmanned aerial vehicles (UAVs) is integrated into outdoor microclimate simulations to enhance the accuracy and precision of the models. The Physiological Equivalent Temperature (PET) index is employed as an evaluation indicator, considering the categorization of PET values into different comfort levels. Additionally, the axial evaluation method is introduced to assess thermal comfort more accurately, reflecting the perceived thermal comfort by individuals. Through a case study in a mixed-use and clear boundary area, the research identifies the variables that influence outdoor thermal comfort and provides design guidelines to enhance spatial thermal comfort. The correlations between the spatial morphology index and PET were analyzed by multiple regression. The findings contribute to the understanding of outdoor thermal comfort in complex urban environments and offer valuable insights for the design and planning of comfortable and sustainable outdoor spaces.

### 1. Introduction

In recent years, there has been a growing interest in the study of outdoor thermal comfort, particularly in relation to the design and planning of urban outdoor spaces [1–3]. The outdoor microclimate is an important factor for people's health and environmental sustainability. It can create a more comfortable environment for people to live and work in and reduce energy consumption. In addition, outdoor microclimates can help protect ecosystems and species by reducing noise, light, and air pollution, provide habitat for animals and plants, and improve water quality by filtering storm water runoff [4,5]. Moreover, outdoor environments are the main places for people to engage in physical activities, and thus the comfort of these environments can have a significant impact on their physical and mental health [6,7]. Various environmental factors such as air temperature, relative humidity, wind speed, and solar radiation can influence outdoor comfort. Therefore, clarifying how these factors impact on outdoor comfort is important for designing comfortable outdoor spaces that can promote human health and well-being while also being environmentally sustainable.

As outdoor thermal comfort is a key factor in enhancing the quality of urban spaces, it is essential to conduct research on different types of outdoor environments. Numerous outdoor thermal comfort studies have been researched on streets [8–13], residential areas [14,15], green parks [16,17], and schools [18,19]. It is crucial to investigate the thermal comfort of mixed-use spaces to deepen our understanding of the various factors that affect outdoor thermal comfort, including environmental parameters and urban features. Researches on outdoor thermal comfort typically focuses on mixed-function spaces [20–23] usually serve multiple functions, such as leisure, entertainment, education, and sports. These spaces often exhibit multiple terrains and urban features, such as buildings, roads, greenery, which also affect the thermal comfort. Understanding the nature and mechanism of outdoor thermal comfort is crucial in designing and improving urban spaces. Moreover, spaces with clear boundaries usually have minimal interfering factors such as traffic, industrial noise, and pollution sources, making them ideal for experimental research, which can deepen the understanding of the nature and mechanism of outdoor thermal comfort [24,25]. At the same time, clear-boundary spaces are often planned and designed artificially, which makes it easier to improve the thermal comfort of the space through de-

\* Corresponding author.

E-mail address: [smiao@qut.edu.cn](mailto:smiao@qut.edu.cn) (S. Miao).

sign measures, thus enhancing the quality and sustainability of urban spaces.

It can be challenging to comprehensively evaluate the outdoor thermal comfort of an entire urban area through point measurements due to the complex and heterogeneous nature of urban microclimates. Some scholars have carried out outdoor scale-down models [26–28], such as ENVI-met. As the most extensively used simulation tools, ENVI-met was employed to visualize the outdoor microclimates. Existing research often uses maps or drawings to obtain and process basic data when building scenario models using ENVI-met. In addition, the constructed physical environment may differ from the drawings, making it difficult to achieve accurate measurement. Some studies also use satellite images and digital elevation models to obtain more detailed terrain and vegetation information in order to more accurately simulate the meteorological environment of actual scenarios [10,29]. However, with the low resolution, satellite images and digital elevation models are difficult to keep up-to-date with actual measurements which may affect the ability to accurately construct the scenario model. Unmanned aerial vehicles (UAVs) can carry high-definition cameras to achieve precise measurements of ground elevation, terrain features, building height and shape, thus providing high-precision scenario data. Using UAVs for on-site measurements as the basis for ENVI-met scenario modeling can provide high-precision scenario information while ensuring time efficiency for actual measurements.

In order to accurately evaluate outdoor thermal comfort, it is crucial to not only collect accurate data for the simulation model but also to identify appropriate evaluation indicators. There are more than 100 thermal indices have been subsequently proposed [30]. Chen and Ng (2012) pointed out that the Predicted Mean Vote (PMV) based steady state model is not suitable for short-term outdoor thermal comfort assessment by reviewing the existing studies [31]. PET is a value that represents the balance of the human body's heat budget and core temperature. PET takes into account the human body's thermoregulation, making it more suitable for the evaluation of outdoor thermal environments. Fazia used the new indicator PET for microclimate assessment of street environments in a study of the impact of outdoor thermal comfort on spatial morphology indicators of streets in Ghardaia and Freiburg [32,33]. Primarily designed for unsteady outdoor environments, based on the physiological energy balance in the human body, PET is derived from the Munich Energy Model for Individuals (MEMI). These studies have identified that street layout parameters such height to width ratio, orientation, and other factors are closely related to PET. Yahia et al. (2018) used ENVI-met to simulate the outdoor microclimate of four built-up spaces with different morphologies and used the degree of decreased PET unit ( $^{\circ}\text{C}$ ) to quantitatively evaluate the outdoor thermal comfort improvement under different optimization scenarios [34]. Fiorillo et al. (2023) used an urban-scale study conducted in Prato, Italy, to correlate PET with thermal perception to evaluate urban land use layout, showing that PET is suitable for understanding thermal stress in the human body [35]. Ren et al. (2022) estimated PET in 183 cities in China over a 26-year period for thermal comfort evaluation and analysis of evolution patterns, further clarifying the application of PET in urban spatial evaluation, emphasized the applicability of PET in capturing human perceived temperature and comfort [36]. Generally, PET values can be classified into several comfort levels, such as less comfortable, moderately comfortable, and highly comfortable. By calculating the proportion of each comfort level, the overall comfort level of the entire area can be obtained. When evaluating the comfort level of the entire area, it is recommended to use the axis as the evaluation index since it is usually where people frequently move around and therefore has a greater impact on people's thermal comfort level. By statistically analyzing the PET values along the axis, average PET value, maximum PET value, and the proportion of comfortable time along the axis can be obtained as the indicators to evaluate the thermal comfort level along the axis. This evaluation method can accurately reflect the actual thermal comfort level perceived by people.

Many studies have been conducted on this topic, using various methods and tools to assess and analyze the thermal conditions of outdoor environments. However, the development of accurate and reliable models for predicting outdoor thermal comfort remains a challenge, particularly in complex urban environments where numerous factors interact to influence thermal conditions. In order to address this challenge, this study employed UAVs to acquire the high-resolution remote sensing data and advanced modeling. Take a mix-uses and clear boundaries area in temperate region as studied location to assess the outdoor thermal comfort and identify the variables influencing of the spatial factors on outdoor thermal comfort. The contributions are as follows.

1. Integrated the high-precision data from unmanned aerial vehicle into the outdoor microclimate simulation. This integration allows for a more detailed and accurate representation of the outdoor environment, enabling a comprehensive analysis of thermal conditions across the university campus.
2. Propose utilizing axial evaluation to assess thermal comfort more accurately, reflecting the actual perceived thermal comfort by individuals. Axial evaluation takes into account individual perceptions and experiences of thermal comfort, ensuring a more human-centric approach to evaluating outdoor thermal conditions.
3. Explored the influence of well-defined boundary spaces on outdoor thermal comfort and provided design measures to improve spatial thermal comfort. By carefully examining the influence of these spaces on microclimates, valuable insights were gained into how the design and layout of urban spaces can significantly affect thermal comfort.

By achieving these contributions, this research enhances the accuracy of outdoor microclimate simulations and thermal comfort assessments. Through a holistic approach that integrates advanced data collection, human-centered evaluation, and spatial design considerations, this study offers valuable knowledge to support the creation of more pleasant and adaptive outdoor spaces for the university campus.

## 2. Materials and methods

The university campus is a comprehensive space that integrates various activities such as learning, living, and recreation. Additionally, the boundaries of a campus are often defined by physical structures, resulting in less disturbance from external noise. This research focuses on studying outdoor thermal comfort within the context of a university campus, aiming to provide scientific evidence and design guidance for improving the campus environment and thermal comfort.

### 2.1. Studied location

Qingdao city is located in the southeastern region of the Shandong Peninsula. The geographical coordinates are  $35^{\circ}35'$  to  $37^{\circ}09'\text{N}$  and  $119^{\circ}30'$  to  $121^{\circ}00'\text{E}$ . This university is located in a temperate monsoon climate. The university campus investigated in this study covers an area of approximately 50 ha and is located in the built-up environment of the city of Qingdao, with central coordinates of 120.20 E and 39.975 N. Its construction was completed in 2020, and the layout of the university campus is shown in Fig. 1. The buildings on this campus are mostly arranged in rows, and the faculty area, central-square, teaching and research areas, and student dormitory living area are distributed from south to north, while the student dormitory living area is also distributed in the eastern and western areas of the campus. The main axes are usually the places where people frequently engage in activities. Therefore, evaluating the main axes accurately reflects the actual thermal comfort level perceived by people when evaluating the overall comfort of area. Students and teachers often engage in outdoor activities for extended periods, such as outdoor exercises and attending classes. Analyzing the main axes can help them better understand the thermal comfort conditions and choose suitable times and locations for

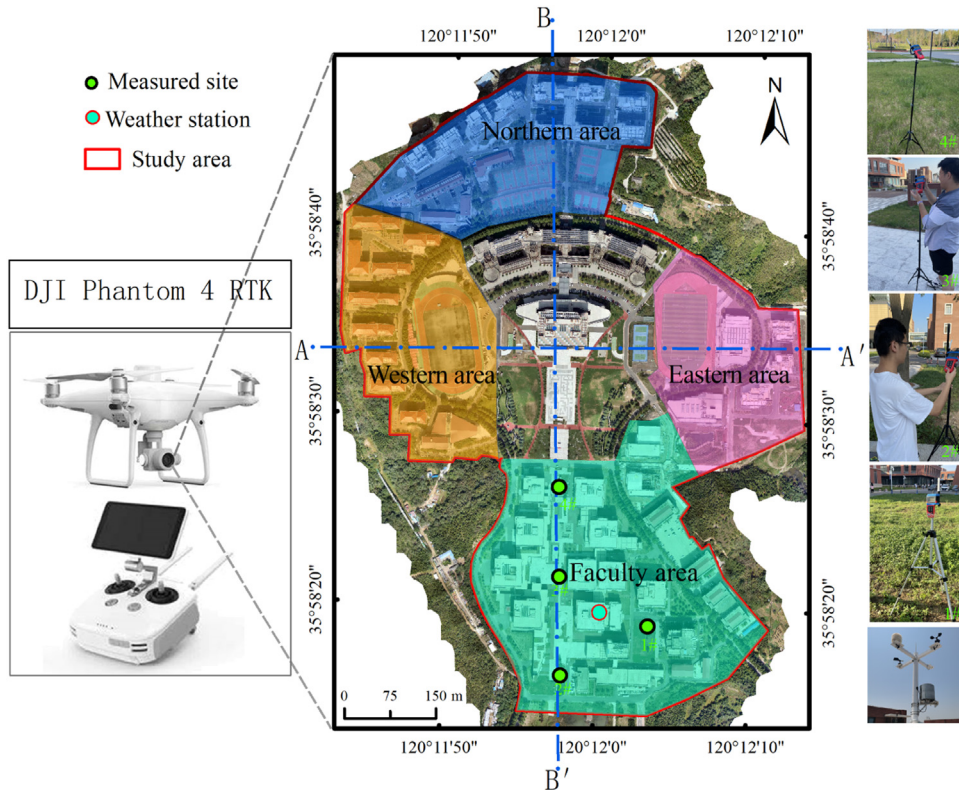


**Fig. 1.** High-precision image map of study area.

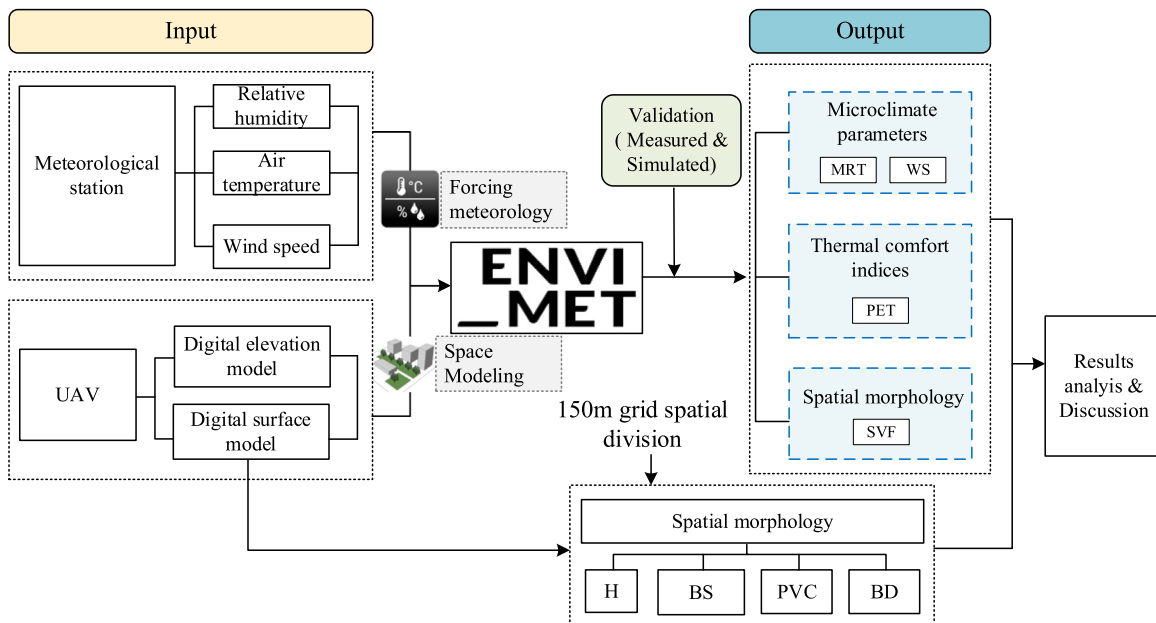


**Fig. 2.** Flowchart of this study.

outdoor activities, thereby avoiding any adverse effects on their physical health due to poor thermal comfort. The two main axes are the east–west axis (A–A') and the north–south axis (B–B'), as shown by the blue lines in Fig. 1. The distance between the east and west edges of the study area is approximately 900 m, and the A–A' axis crosses the library, square, playgrounds, and dormitories. The north-to-south direction is approximately 1200 m. The B–B' axis, spanning from south to north, passes through different spatial forms, such as the teaching and research area, square, teaching buildings, sports fields, and dormitory area.

The research steps and process are shown in Fig. 2. First, a digital surface model (DSM) of the Qingdao University of Technology campus was obtained with a high-precision unmanned aerial vehicle (UAV) aerial survey, which provided accurate elevation data and high resolution image (0.5 cm/pixel) for outdoor space microclimate simulation and building spatial morphological indices of the campus. Then, the achieved high-precision spatial data by UAV aerial survey is input into ENVI-met as the space model. Simultaneously, the measured air temperature ( $T_a$ ) and relative humidity (RH<sub>u</sub>) is used to validate the ENVI-met model performance at 1.5 m by setting four collection sites, the locations

**Table 1**  
Specific information of the UAV.

Performance parameter	Specific parameter value
UAV type	DJI Phantom4 RTK
Image sensor	1 inch CMOS; effective pixels 20 million
Lens:	FOV84°
Focal length	8.8 mm
Aperture	f/2.8-f/11; with autofocus; focus distance 1 m -∞
Coordinate system	World Geodetic System 1984

of which are given in Fig. 2. At last, this study quantitatively assess the outdoor thermal comfort of the university campus based on the microclimate simulation results.

## 2.2. On-site measurements

An aerial survey of the study area was performed using a high-precision UAV to acquire data. The specific UAV information is provided in Table 1. A high-precision orthophoto map (Fig. 1) and DSM of the region were synthesized by DJI Terra, and the images were clipped and transformed in Arc-GIS. A digital elevation model (DEM) representing the study area was combined to calculate the information required by the ENVI-met space model, such as the heights of buildings and vegetation on the university campus. The World Geodetic System (WGS) 1984 scheme was adopted as the UAV coordinate system to obtain digital information on the terrain, roads, buildings, and vegetation (Fig. 3a). The lowest point in the area was regarded as 0 m, and the elevations of the terrain, buildings, and trees were converted into relative heights (Fig. 3b).

Qingdao is affected by both high temperatures in summer and cold air fronts in autumn, resulting in higher temperatures in September, with an average temperature of around 20 °C and daytime maximum temperatures exceeding 30 °C. The actual measured highest temperature for the day reached 30.6 °C. Due to its coastal location, Qingdao is prone to the formation of fog due to the moisture from the ocean, leading to relatively high humidity in September. This can have a cer-

**Table 2**  
Parameters of the university campus weather station.

Parameter	Range	Accuracy	Units
Relative humidity	0–100	0.1	%RH
Air temperature	-40–80	0.1	°C
Wind speed	0–30	0.1	m/s
Wind direction	16 direction/360°	1	°
global radiation	0–1500/0–2000	1	W/m <sup>2</sup>

tain impact on outdoor thermal comfort. Students and teachers have ample time for activities on campus, and the simulation results can better reflect the variations in thermal environment at different times on campus. The measurement was carried out from 16:00 on September 29 to 12:00 on October 1. Typical weather conditions were selected, with no rainfall, typhoons, or other extreme weather conditions on the three days before and after. Considering the semester schedule of the students, the 24 consecutive hours on September 30 were taken as the typical weather condition for the assessment and analysis of the thermal environment of the campus. The meteorology parameters ( $T_a$  and RHU) were measured by a handheld temperature and humidity instrument (JT08) with accuracy of 0.1 °C and 0.1% RH, recording data every minute. Average the data recorded every minute for an hour to get the hourly value. Focus on the impact of the spatial morphology factors on the university campus outdoor microclimate, this influence is most obvious when the weather was sunny. It is necessary that no humid airflow, rain, typhoon, or other extreme weather occurred within 3 days before or after the measurement day. The  $T_a$  and RHU measured devices set at a height of 1.5 m and recorded every minute. As Fig. 1 shows, site 1# is located in the green space enclosed by a four-sided building, site 2# is located under a tree, site 3# is located in a square, and site 4# is located in a green space with buildings on both sides. The data from the campus weather stations are also recorded as regional weather data. The location of this weather station is shown in Fig. 1, and the parameters of the university campus weather station are shown in Table 2.

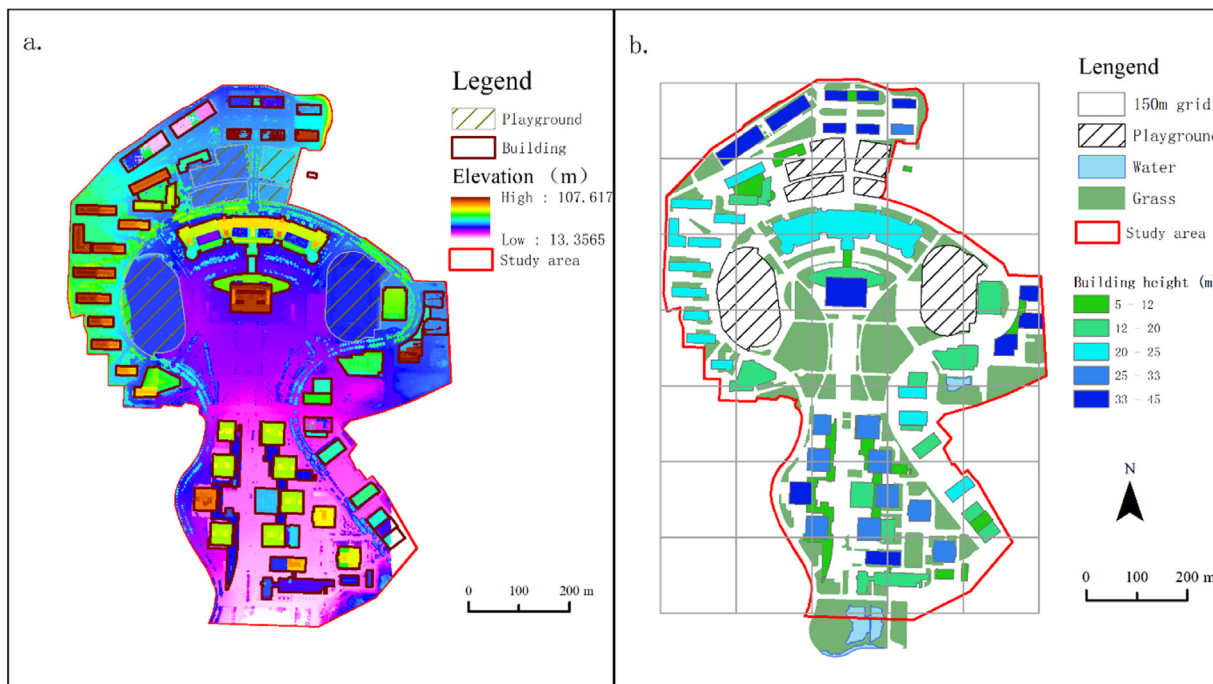


**Fig. 3.** Digital surface model and layout of study area(a. is digital surface model of QUT and b. is layout of QUT).

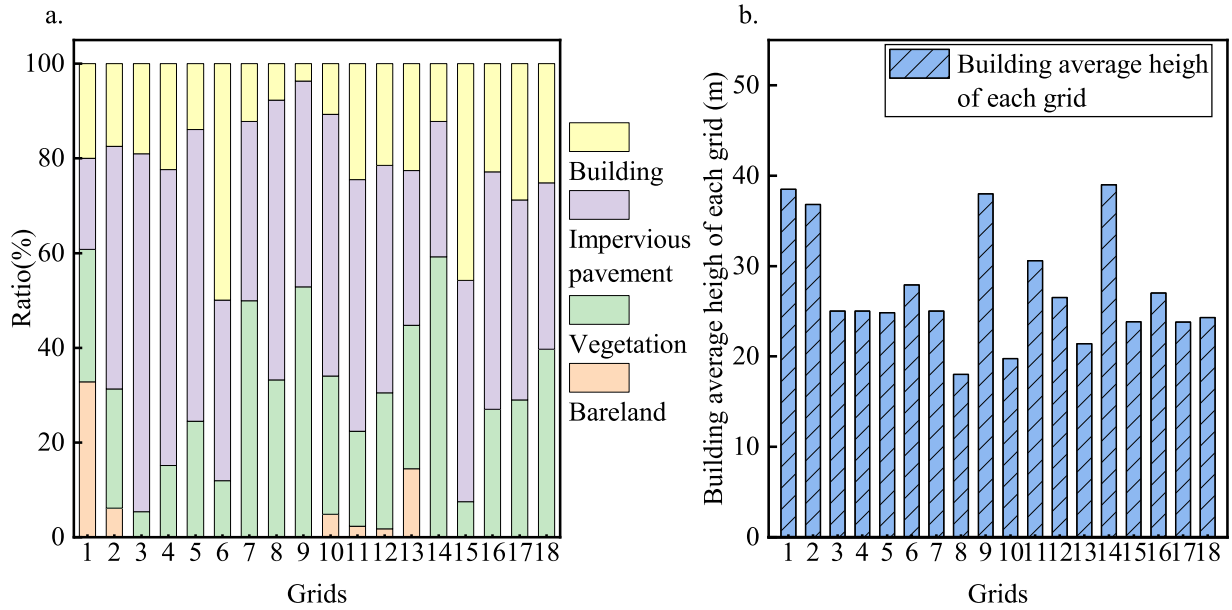


**Fig. 4.** Bar chart of vectorization calculation results in each grid (a. is a bar stacking chart of the percentage of buildings, roads, green areas, and bare land; b. is the average building height).

**Table 3**

Calculation methods and meanings of the spatial morphology indices.

Indices	Formula	Indicator description	Graphical description	Software
SVF	$SVF = 1 - \frac{\sum_{i=1}^n \sin \gamma_i}{n}$	Proportion of the sky at the specified location that occupies the upper hemisphere		ENVI-met
BD	$BD = \frac{S_{building}}{S}$	Percentage of building footprint to total area		Arc GIS
PVC	$PVC = \frac{S_{green}}{S}$	Percentage of green area to total area		
BS	$\frac{H_{avg}}{BD}$	Overall building scale		

### 2.3. Spatial morphology factors and thermal comfort index

The different spatial forms can change the heat distribution and air flow in the surrounding environment, leading to variations in the PET due to the combined effects of air flow, shading and solar radiation, as well as surface temperature. According to the results of some previous studies [37,38], the microclimate of urban locations is mainly influenced by the land cover of the surrounding hundreds of meters. Therefore, in our study, a 150 m grid covering the study area was used to calculate the building coverage, vegetation coverage, and building scale. Based on the DSM and image maps acquired by UAV, the study area was divided into 150-m grid areas in Arc GIS to calculate the spatial morphological indices within each grid. As shown in Fig. 4a, vectorization of high-precision images are performed to calculate the percentage of buildings, roads, green areas, and bare lands in each grid. The average height of buildings in each grid is also calculated based on DSM data, and the specific results are shown in Fig. 4b.

Table 3 shows the calculation methods and meanings of the spatial morphology indices, percentage vegetation cover (PVC), and percentage of buildings coverage within the each grid (BD) calculated with

Arc GIS. The average building height to BD ratio represents the overall building scale (BS); to calculate this ratio, the height of each building was measured from the DSM in Arc GIS, and the building footprint area percentage was measured using Arc GIS [39]. Sky View Factor (SVF) is an important comprehensive spatial morphology factor that has a direct impact on solar radiation exchange. It is a dimensionless quantity ranging from 0 (no visible sky) to 1 (free hemisphere) that represents the geometric ratio of a specific place and expresses the fraction of the overlying hemisphere occupied by the sky [40,41]. The size of the SVF was directly influenced by the surrounding buildings, trees, and other structures with different building spaces. This also indicates that the size of the area exposed to the sky and thus receiving solar radiation is variable, thus further affecting the microclimate of the study area. The shadows from buildings and the SVF affect the microclimate by approximate mechanisms; both shield the land surface from solar radiation, which in turn changes the microclimate of the outdoor environment.

PET is appropriate for assessing outdoor thermal comfort because of it integrates the effects of shortwave and longwave radiation fluxes on body heat balance in an outside atmosphere [42]. According to China's building climate division, Tianjin and Qingdao are located in the same

**Table 4**  
Input parameters for the ENVI-met inputting.

Parameter configuration	Input parameters	ENVI-met
General setting	Space model area <sup>1</sup> $x \times y \times z$ size Position on earth Time zone Simulation start date Simulation start time Total simulation time	300 × 400 × 25 3 m × 3 m × 5 m 120.20 E 35.97 N CET/GMT +8 September 29, 2021 00:00 48 h
Initial meteorological conditions	Wind speed measured in 10 m height Wind direction(deg) <sup>2</sup> Specific humidity at model top (2500 m, g/kg) Roughness length Specific humidity at 2500 m	2.94 m/s 202.5° 8.0 0.1 7 g/kg

<sup>1</sup> The space size of university campus is 900 m × 1200 m × 125 m.

<sup>2</sup> (0=from North...180=from South).

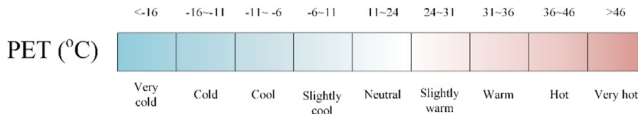


**Fig. 5.** Thermal benchmarks of human subjective thermal sensation.

climate division, and both are located in cold regions; thus, the evaluation was carried out with reference to the PET thermal sensation scale of Tianjin [43]. The subjective thermal sensation was separated into nine levels ranging from very cold to very hot (Fig. 5). When the PET exceeds 24 °C, humans feel slightly warm, and when it exceeds 31 °C, they feel warm. According to the thermal comfort benchmarks of Tianjin, these human subjective thermal sensation and heat stress benchmarks are shown in Fig. 5. The influence of spatial morphology on human thermal comfort can be better understood by comparing the relationship of urban form indicators on PET.

### 3. Results

#### 3.1. Modeling and validation of ENVI-met

High-precision data achieved by UAV to construct the space model, plants, and the materials of buildings and soil. The simulated date was September 30th, 2021, and the simulation time spanned from 00:00 to 23:00. The start time of the simulation was fixed to 00:00 on September 29th, 2021 in addition to avoiding the effects of startup (24 h). The basic meteorological parameters are input with the available data of university weather station. A list of all the microclimate parameters input into the simulation model is shown in Table 4. PET is calculated with meteorological data and human body parameters. The index was calculated for a 22-year-old man that is 1.75 m tall and 70 kg in weight, with a metabolic rate of 169.98 Wm<sup>-2</sup> and clothing insulation of 0.8 clo.

By comparing the root mean square error (RMSE) of the simulated  $T_a$  and the field  $T_a$  at the same location, the ENVI-met model's validity is assessed in this study. The RMSE is a measure of the difference between values (predicted and actual) simulated by a model. The lower the value, the better the model fits the data. A higher RMSE value indicates that the model is not as good at predicting the data. On September 30, 2021, from 00:00 to 23:00, the hourly measured and predicted  $T_a$  were used to validate the ENVI-met model. The 24-h simulated  $T_a$  by ENVI-met are compared with the data measured at the 4 points. The results are shown in Table 5. As Fig. 6 shown, the measured and the simulated  $T_a$  - RMSE on the same locations is 1.65.

A review of the literature on outdoor microclimate studies using ENVI-met over the past 10 years shows that many scholars have used  $R^2$  and RMSE as measures to evaluate the accuracy of ENVI-met model simulations [8,42,44–55]. Fig. 7 collates the error coefficients ( $R^2$  and

**Table 5**

Results of ENVI-met model performance based on measurement and simulation.

Measured point	$T_a$ - $R^2$	$T_a$ -RMSE
1#	0.890	1.86
2#	0.917	0.55
3#	0.888	1.91
4#	0.859	1.87
Total	0.883	1.65

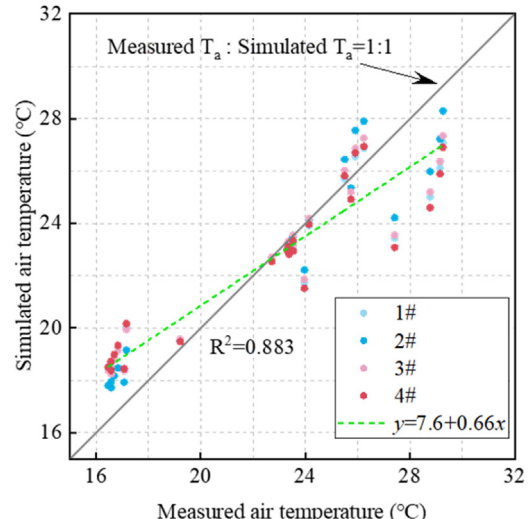


**Fig. 6.** Thermal benchmarks of human subjective thermal sensation.

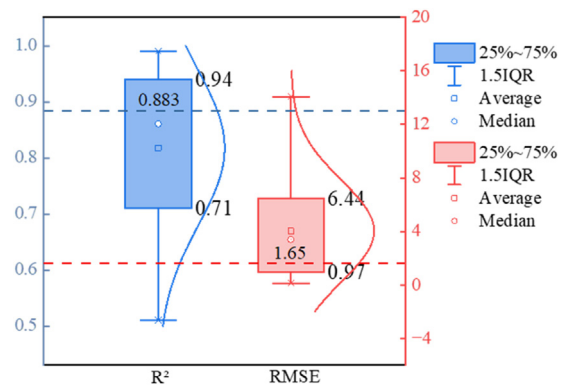


**Fig. 7.** Error coefficients ( $R^2$  and RMSE) from research within the last decade.

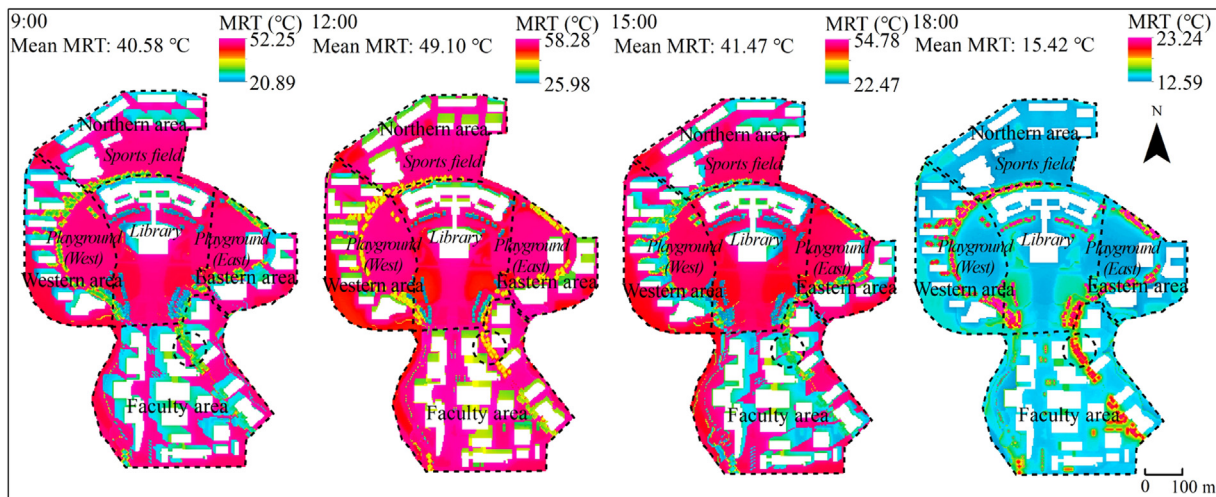


**Fig. 8.** MRT Spatial distribution of study area at 09:00, 12:00, 15:00 and 18:00.

RMSE) from these studies to allow us to perform simulations with a measured value-validation process. As Fig. 7 shows, the  $R^2$  and RMSE values were in the allowable error ranges, indicating that ENVI-met can simulate the urban microclimate very well.

### 3.2. Simulated results analysis

Mean radiant temperature (MRT), wind speed (WS), and PET simulation results at a 1.5-m height at 9:00, 12:00, 15:00, and 18:00 were extracted to assess and analyze the outdoor comfort conditions of the campus. The two-dimensional distribution data were output from the LEONARDO module of ENVI-met and visualized with Arc GIS. MRT is used to describe a hypothetical environment in which the rate of heat transfer from the human body is equal to heat transfer in the actual. The effect of MRT on human comfort is mostly due to the effect of the surrounding object surface temperature on the intensity of radiation heat dissipation from the human body. When there is a temperature difference between objects surface and the human body, the human body will produce a sense of cold and heat radiation through radiative heat exchange. Both too-low and too-high MRT will increase heat exchange between the body and its surroundings, forcing its own thermoregulatory mechanism to work for an extended period of time and creating systemic diseases.

Fig. 8 depicts the MRT distribution at 9:00, 12:00, 15:00, and 18:00. The mean MRT values at 9:00, 12:00, 15:00, and 18:00 were 40.58 °C, 49.10 °C, 41.47 °C, and 15.42 °C, respectively. Because the sunrise time is 05:52 and the sunset time is 17:44, the average MRT in the 18:00 region is lower when compared to the MRT at 9:00, 12:00, and 15:00. MRT values are lower in shaded regions of buildings and trees (blue and green MRT values) and stronger in open sports fields and sunny sides of buildings (red MRT values). In addition, the shadows cast by buildings move with the angle of the sun; therefore, locations with lower MRT frequencies move. For example, when comparing the North Zone (building height of approximately 40 m) and the West area (building height of approximately 25 m), the lower MRT area in the West area is less than that in the North area due to the higher building height in the North area increasing the shaded area and decreasing the MRT. The university campus tree canopy can help to shade sunlight, preventing daytime shortwave radiation and longwave radiation at night. The region under the trees (e.g., circle in Fig. 8) has a lower MRT value during the day than the surrounding unshaded area but a greater MRT value at night than the unshaded area.

Fig. 9 shows the wind speed spatial distribution of university campus. The figure shows that the wind speed is higher in the playgrounds

and sports fields, but the wind speed distribution is more stable. However, at the same time, the blockage of buildings such as teaching buildings and dormitory buildings led to lower local wind speeds in the areas surrounding these buildings, which led to relatively large differences in the wind speeds across the campus. Wind speed is more unstable in the northern area, where building density is higher. When the wind hits a building obstacle, it will go around the building and continue in the same direction, and the wind speed will rise at the corner (red underlined area), causing the wind corner effect. The higher and wider the blocked building is, the stronger the effect will be. Furthermore, the narrow tube effect of wind will arise in the passage between high-rise buildings, showing wind speed amplification, and the higher the building's height, the more significant. The influence of the clustered buildings reduces the local wind speed of the outdoor environment, leading to a significant difference. It may be shown that various spatial morphologies influence the change in wind speed in the area.

Fig. 10 shows the PET results distribution of study area. The distributions of the PET were more stable in the open areas of the sports field and square. Relatively low PET values were mainly located on the north side of the buildings and underneath trees, as the buildings and tree canopies reduced the PET values by shielding the land surface from solar radiation; in contrast, relatively high PET values were mainly observed on the south sides of buildings and above unshaded pavement and hard pavement. University campus sports fields are typically designed adjacent to dormitory areas, where large differences in the thermal environment can reduce damage to the body. The environmental wind speed reduces the convective heat dissipation and skin evaporative heat dissipation of the human body, thereby reducing the skin-surface moistness and temperature and impacting thermal sensation. Therefore, excessive wind speeds and large differences in the PET values within the dormitory area could affect the thermal regulation of the human organism following physical exercise, which in turn would affect physical health.

### 3.3. Outdoor thermal comfort analysis

There are numerous areas with little human activity where areas not only add difficulty to analysis and evaluation but also decrease their accuracy. By analyzing and evaluating the PET values along the axial area, targeted improvement measures can be implemented. For areas with high PET values along the axis, measures such as adding shading facilities and increasing greenery coverage can be taken to reduce thermal discomfort and enhance people's comfort. On the other hand, for areas with low PET values along the axis, measures such as adding ventilation facilities and increasing water coverage can be implemented to

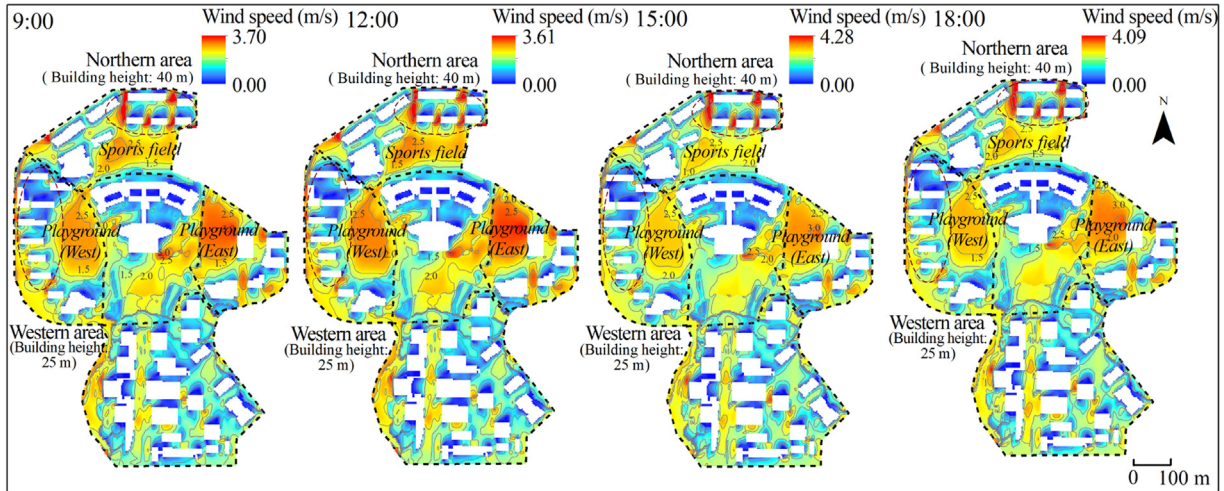


**Fig. 9.** Wind speed distribution of study area (9:00,12:00,15:00 and 18:00).

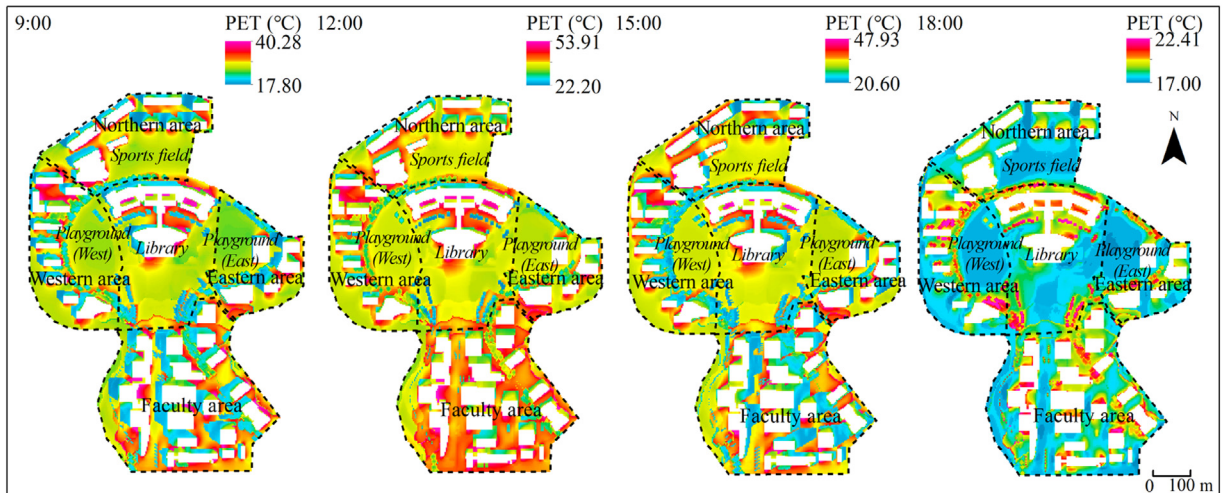


**Fig. 10.** PET distribution of study area (9:00,12:00,15:00 and 18:00).

improve thermal comfort and enhance people's comfort. Therefore, to quantitatively evaluate the outdoor thermal comfort of studied university campus, PET simulation results at a height of 1.5 m at 9:00, 12:00, 15:00, and 18:00 were extracted to evaluate the outdoor comfort level of the campus. According to China's building climate division, Tianjin and Qingdao are located in the same climate division, and both are located in cold regions; thus, the PET evaluations were carried out using the thermal sensation scale of Tianjin.

When the average value of the A-A' (west–east) axis was compared at 9:00, 12:00, 15:00, and 18:00, the PET was highest at 12:00, and the related thermal sensation was highest. Fig. 11 shows that most of the PET temperatures exceeded 31 °C and were located within the "warm" subjective thermal sensation range. Among them, the highest PET value was 35.97 °C, distributed above a road without shade. PET values between 24 and 33 °C were in the "slightly warm" subjective thermal sensation range, with the lowest PET value of 26.74 °C being distributed under roadside trees. When PET values range from 11 to 24 °C, the subjective thermal sensation of the human body is considered "neutral", in a comfortable state; however, along the A-A' (east–west) axis of the campus, an uncomfortable state occurred at 12:00, when the overall temperature was hot. The PET differences between the four periods are 14.82 °C, 9.23 °C, 10.73 °C, and 1.94 °C. The greatest difference occurs at approximately 9:00 a.m. PET, and the smallest difference occurs at 18:00. Fig. 11 presents the PET distributions on the east–west campus

axis. The figure shows that the PET values on this axis show different distribution trends along with the axial space changes. Throughout the building area, the PET values change significantly. In contrast, these variations are smaller and more stable when crossing the squares and playgrounds. These results indicate high levels of thermal discomfort along most of the A-A' (east–west) axis.

When the average value of the B-B' (north–south) axis was compared at 9:00, 12:00, 15:00, and 18:00, the PET was highest at 12:00, and the related thermal sensation was also highest. Fig. 12 shows the distributions of PET along the north–south axis at 12:00. The PET values along this axis show different distributions as they cross different spaces. According to Fig. 12, the PET values along this axis mostly exceed 31 °C, with the highest PET, reaching 37.12 °C, distributed above an unshaded road. PET values between 24 and 33 °C are considered to be within the subjective thermal sensation range of "slightly warm", and the lowest obtained PET was 25.6 °C, distributed in the shaded areas of a building. PET values between 11 and 24 °C are considered "neutral", meaning comfortable, while these values were uncomfortable along the A-A' (east–west) axis of the campus at 12:00 noon. The PET differences between the four periods are 10.81 °C, 10.52 °C, 11.10 °C, and 2.25 °C. The greatest difference occurs at approximately 9:00 a.m. PET, and the smallest difference occurs at 18:00. The PET difference is greater than the A-A' (east–west) axis for all periods except for 9:00, which is smaller than the W-E axis.

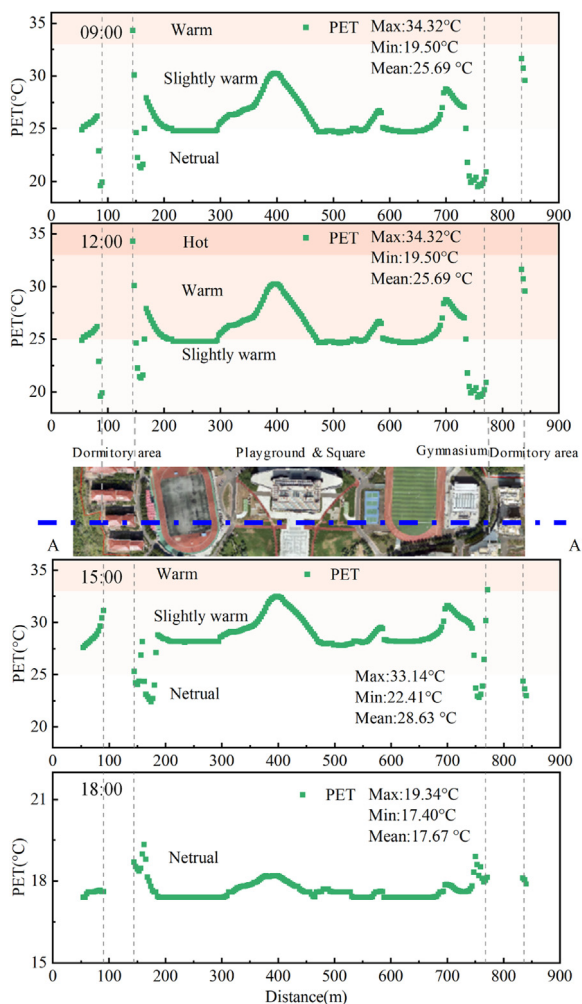


Fig. 11. PET of A - A' (west-east) axis.

Outdoor spaces with relatively dense buildings affect outdoor comfort. The results of the study show that most of the studied spaces had relatively high thermal comfort. Therefore, it is recommended to improve their thermal comfort by optimize the outdoor area layouts. When the mean values of the two axes for the four periods are compared, it is discovered that the mean value of the B-B' axis at 12:00 is greater than the mean value of the A-A' (east-west) axis. Then, the mean values of the two axes are equal at 18:00, and the mean values at 9:00 and 15:00 are smaller than the mean value of the A-A' (east-west) axis. This indicates that the overall PET of the A-A' axis is greater than that of the B-B' axis. The outdoor spaces crossed along the A-A' (east-west) axis mainly included playgrounds, green areas, and squares, while the south-north axis crossed the faculty area, teaching area, and dormitory area, areas in which buildings are more concentrated. Table 6 shows the findings of a statistical analysis of the proportion of subjective heat sensation on the B-B' (north-south) axis and the A-A' (east-west) axis for PET values corresponding to 09:00, 12:00, 15:00, and 18:00.

According to Table 6, at 12:00, the subjective thermal sensation on both axes was at its peak. The thermal sensation was the weakest at 18:00, and the distribution trends at 09:00 and 15:00 were similar. When the proportion of thermal sensation is compared across the four time periods, the proportion of "slightly warm" of the B-B' (north-south) axis is smaller than that of the A-A' (east-west) axis at 9:00 and 15:00 and at 12:00. The thermal sensation comfort of the B-B' (north-south) axis is stronger than that of the A-A' (east-west) axis, and at 18:00, the thermal sensation along the B-B' (north-south) axis is similar to that along the A-A' (east-west) axis. Generally, both the mean PET and the proportion of subjective thermal sensation of the B-B' (north-south) axis are smaller than those of the A-A' (east-west) axis; thus, it is generally shown that the B-B' (north-south) is more comfortable than that of the A-A' (east-west) axis.

## 4. Discussion

### 4.1. Influence of spatial morphology on the PET

The PET simulations indicated that different spatial morphologies influence the microclimate of the study area, in turn affecting the comfort level of the study area. Moreover, this influence differs signif-

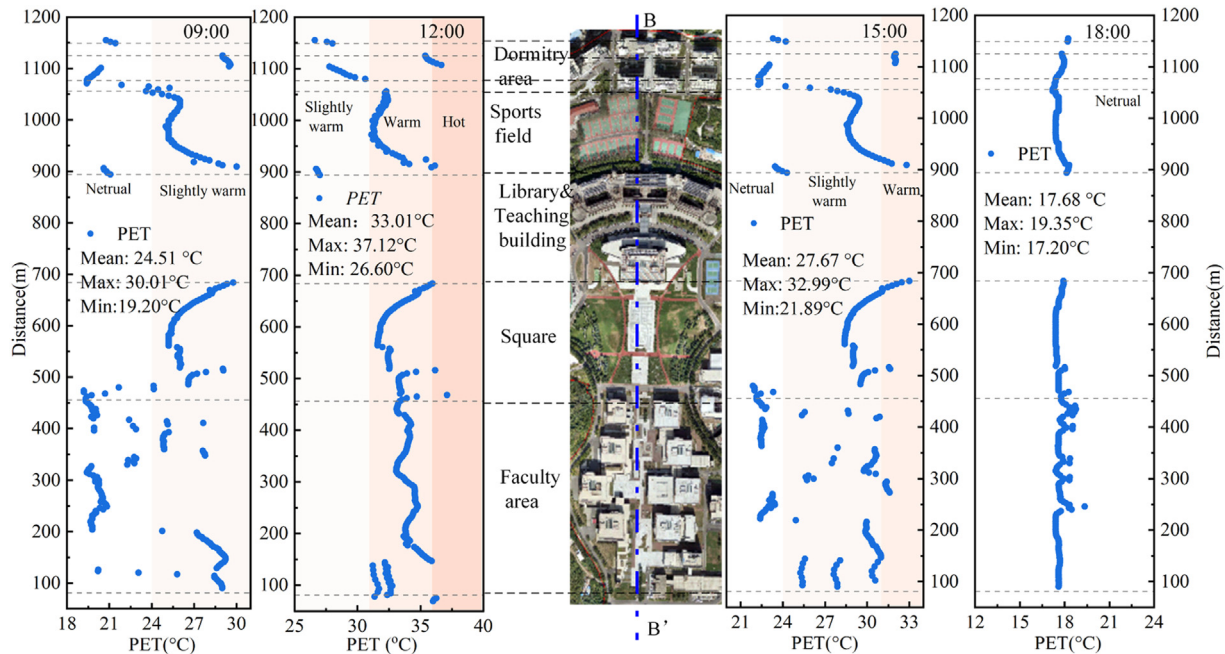


Fig. 12. PET of B-B'(south-north) axis.

**Table 6**  
Results of human subjective thermal sensation.

Axis	Time	Human subjective thermal sensation			
		Neutral	Slightly warm	Warm	Hot
A-A' (west–east)	09:00	8.40%	91.59%	0	0
	12:00	0	16.89%	83.11%	0
	15:00	5.31%	94.69%	0	0
	18:00	100%	0	0	0
B-B' (north–south)	09:00	35%	65%	0	0
	12:00	0	6.79%	90.36%	2.86%
	15:00	25.36%	74.64%	0	0
	18:00	100%	0	0	0

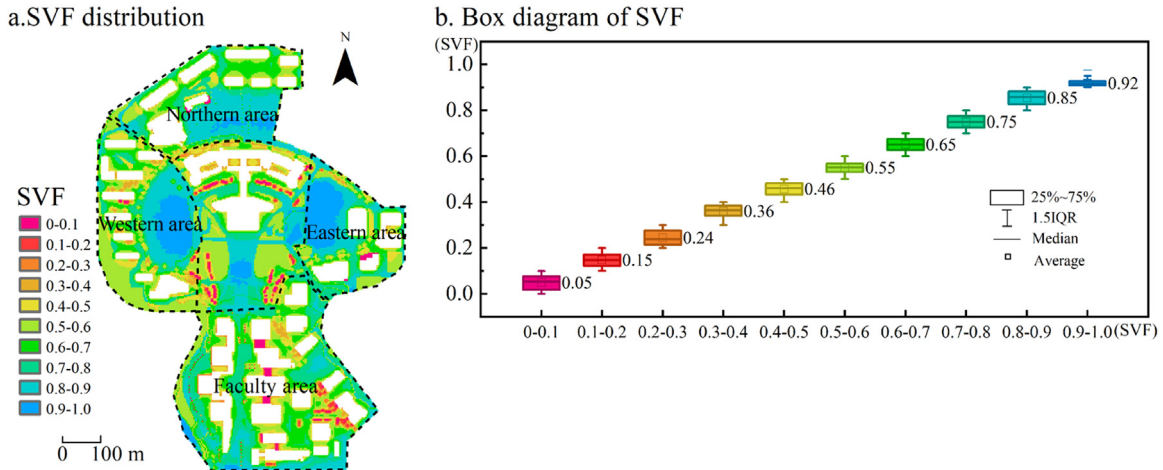


Fig. 13. SVF data distribution (a. spatial distribution b. box diagram of each interval).

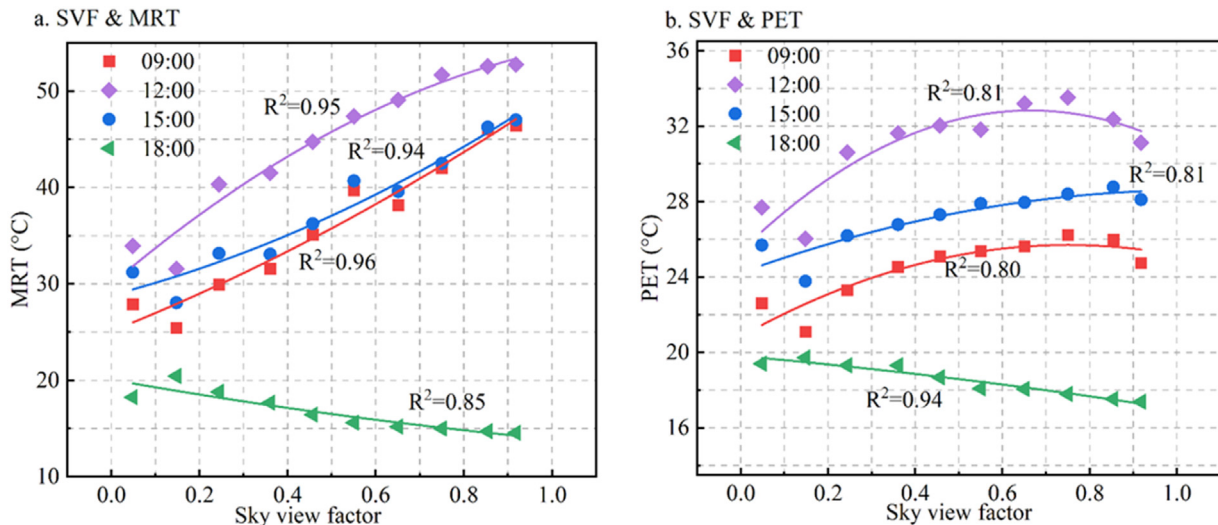


Fig. 14. Scatter diagram of the relationship between SVF against PET and MRT.

icantly under different spatial morphological characteristics. To further clarify the effects of different spatial morphological characteristics on comfort, the effect of spatial morphology on comfort was further explored.

Based on the simulated campus microclimate data, the relationships between the SVF and MRT and PET were studied. SVF values are between 0 and 1. The SVF values calculated by ENVI-met for the campus space were divided into 10 intervals (0–0.1, 0.1–0.2, 0.2–0.3,..., 0.9–1). Fig. 13a depicts the spatial distribution of the SVF, while Fig. 13b depicts the distribution of values within every interval. The average SVF values in each interval and the corresponding MRT and PET values were cal-

culated. Fig. 14 shows scatter diagrams of the comparisons between the PET, MRT, and SVF. According to Fig. 14a, the correlation coefficient ( $R^2$ ) values between the SVF and MRT were 0.95, 0.94, 0.96, and 0.85. at four different times, respectively. Fig. 14b's SVF and PET correlation coefficients  $R^2$  were 0.81, 0.81, 0.80, and 0.94 at four different times, respectively. This shows that variations in SVF have a significant impact on MRT and PET. These values indicate strong positive correlations between them at 09:00, 12:00, and 15:00, and MRT and PET increased with increasing SVF. Different patterns were present in each of the four periods. Positive trends were seen at 09:00, 12:00, and 15:00, but at 18:00, the SVF showed a negative correlation that was in opposition to

**Table 7**  
Results of multicollinearity.

Independent variables	VIF			
	9:00	12:00	15:00	18:00
WS	2.113	2.015	1.712	2.001
BS	1.674	1.671	2.042	1.664
PVC	2.141	2.142	2.943	2.020
BD	3.456	3.352	1.665	3.216

that of MRT and PET. Shading can reduce radiant heat and temperature on a building's surface or pavement. A higher SVF means that more solar radiation is received during the day, and a higher SVF leads to a higher MRT. The MRT decreases as the SVF increases because there is less obstruction to longwave radiation release at night. The SVF is closely connected with the outdoor air temperature, according to studies done in Brazil [56], Singapore [57], Iran [58], and other locations [59]. The building morphology affects the SVF value, which further affects the outdoor comfort level. Fig. 14b illustrates a decreasing trend in PET when SVF exceeds 0.75 in 09:00, 12:00 and 15:00. In situation where the sky is very open, the wind speed tends to be stronger, which can result in feelings of coldness and discomfort. Despite the air temperature may not being particularly high during such instances, the impact of strong winds leads to decreased perceived PET values. Therefore, when designing and planning outdoor environments on campus, strategies such as the use of trees and sunshades can be employed to reduce direct solar radiation, while increasing greenery and implementing windbreaks can help lower wind speeds.

Through different layouts, campus buildings, roadways, and green spaces create different spatial forms that in turn lead to various microclimates. To further clarify the mechanism of analyzing the effect of morphological indicators on PET, a quantitative analysis was performed using multiple linear regression. PVC, BD, and BS are used as independent variables, and PET was used as the dependent variable in a multiple regression model to analyze the influence of spatial morphology on PET. Considering that PET is a comprehensive indicator of the thermal comfort that takes into account multiple environmental parameters, the inclusion of wind speed as an independent variable in the regression model ensures its effectiveness. Based on this effective model, the individual contributions of three morphology indicators (BS, PVC, and BD) to PET are quantified by their coefficients. This analysis aimed to further clarify the influence mechanism of spatial morphology on thermal comfort indices in outdoor spaces. Then, the mean values of the morphological indicators and PET within each zone were calculated, and the data in the grids that completely covered the campus were analyzed. The influence of spatial morphology on human thermal comfort can be better understood by comparing the relationship of urban form indicators on PET. The four independent variables were tested for multicollinearity using the variance inflation factor (VIF) as the index, and the results are shown in Table 7. Usually, VIFs greater than 5 indicate critical levels of multicollinearity in which the coefficients are poorly estimated. The results show that the VIF values for all variables were < 5, indicating an acceptable level of multicollinearity.

The results of the multiple linear regression analysis are shown in Table 8. The regression model results for PET as the dependent variable, where the R<sup>2</sup> ranged from 0.608 to 0.722 and the significance are smaller than 0.05, it indicates that the model regression was effective. The absolute values of the standardized coefficients for the three morphological indicators presented in Table 8 provide an indication of the extent to which they influence PET values. A larger absolute value of the standardized coefficient suggests a more prominent impact. Specifically, the morphological indicator BD exhibits a substantially higher influence on PET values at 12:00, 15:00, and 18:00 compared to the indicators BS and PVC. The absolute values of the standardized coefficients for BD are 0.361, 0.374, and 0.286, respectively. These findings

clearly demonstrate that BD, among the morphological indicators, has the most pronounced effect on PET.

#### 4.2. Comparison with previous studies and optimiziton strategies

Previous studies related to the assessment of thermal comfort on university campuses have mainly focused on quantifying subjective thermal comfort from objective indicators. Baruti et al. (2020) conducted on university campus have mainly focused on quantifying subjective surveys to assess the thermal neutrality of outdoor environments in warm-humid tropical Tanzania [60]. Similarly, Xue et al. (2020) studied outdoor thermal environmental comfort on Shanghai campus and obtained quantitative relationships (R<sup>2</sup>: 0.42 and 0.62) between PET and UTCI and human subjective thermal sensation [61]. Xue et al. (2021) showed that the thermal environment has a significant impact on students' behavioral activities through a measured study of a campus [62]. The study indicated that attendance and non-essential activity levels increase with higher outdoor temperatures when the outdoor environment exceeds 20 °C, highlighting the significant influence of outdoor thermal environment on outdoor activities in campus spaces. Yu et al. conducted measurements in a university campus space in Singapore and confirmed through nonlinear models that SVF, building density, and other morphology variables have an impact on student activities at a set point (2.4 m height) in a tropical area [21,39]. The model confirmed that when the sum of the leaf area index of each species multiplied by canopy area and then divided by the site area (GnPR) increased from 3 to 3.6, Tavg, Tmin, and Tnight-avg decreased by 0.58 °C, 0.25 °C, and 0.83 °C per 0.5 GnPR increment respectively. The aforementioned studies have relied on point measurements for evaluation. However, limited measurement points make it difficult to accurately capture spatial variations. In this study, pedestrian height (1.5 m) data were extracted to evaluate and analyze the thermal comfort of the two main axes of the campus with the highest attendance rate. Furthermore, Sun et al. (2022) [63] conducted a study on typical areas with different urban densities and street layouts and found that SVF had the highest correlation with MRT and PET (Pearson correlation coefficient: 0.42 to 0.68) in summer. Moreover, Deng et al. (2023) [64] conducted measurements in a typical urban area in Guangzhou, China and built regression models of environmental variables for PET with an explanatory power (R<sup>2</sup>: 0.32 to 0.82). They found that SVF and building coverage ratio had a significant impact on the outdoor thermal comfort of urban old and new blocks. The conclusion of this study are consist with the previous mentioned results.

This study conducted research on the influence of spatial morphological on outdoor thermal environment in a representative space with clear boundaries and mixed functions. In urban-scale studies, Gao et al. (2022) analyzed the relationship between 10 urban spatial variables and thermal environment using the GWR model and found that building density and impervious surface ratio had a significant impact on the thermal environment [65]. Additionally, Zhang et al. (2022) [66] investigated the relationship between 17 two-dimensional and three-dimensional spatial morphology indicators and MRT and PET. It was found that building floor area ratio (impact coefficient: -0.809 to -0.877) and tree crown coverage ratio (impact coefficient: 0.243- 0.446) were the most important predictors for PET during the day and at night respectively. This study focuses on typical small-scale spatial research, and its findings

**Table 8**

PET regression model coefficients and results.

Independent variable	9:00		12:00		15:00		18:00	
	Std. coefficients Beta	t						
WS	-0.822	-3.721	-0.7	-4.119	0.637	2.951	-0.940	-5.778
BS	0.371	1.889	0.133	0.862	-0.282	-1.194	-0.141	-0.949
PVC	-0.301	-1.354	0.183	1.045	-0.1	-0.354	-0.170	-1.039
BD	-0.062	-0.219	0.361	1.645	0.374	1.755	-0.286	-1.387
Constant	29.260		35.158		26.695		19.419	
R <sup>2</sup>	0.608		0.756		0.646		0.775	
Adjusted R <sup>2</sup>	0.515		0.699		0.537		0.722	
F	6.585		13.178		5.924		14.636	
Significance	0.002		0.000		0.006		0.000	

are consistent with those of large-scale urban studies. The influence relationship in local spaces can maintain a consistent trend with the overall regional and urban scale. Optimizing local spaces can improve the overall quality of the urban thermal environment. This study demonstrates that optimizing the morphological indicators of buildings can not only improve comfort but also further impact the overall regional morphology, thereby enhancing regional comfort. From the perspective of improving spatial comfort, the following design strategies can be proposed for optimizing campus spatial planning and renovation.

1. University campus sports fields are mostly designed adjacent to dormitory areas, and the optimization of areas with large thermal environment differences can reduce damage to the body. The environmental wind speed affects the convective heat dissipation and skin-evaporative heat dissipation abilities of the human body, thus reducing the skin-surface moistness and temperature; these processes impact thermal sensation. Therefore, the excessive wind speeds and large PET measured in the dormitory area can affect the thermal regulation of the human organism after physical exercise, which in turn can affect physical health. Hence, considering the optimization details for small-scale local spaces, shading installations and trees could be combined with open squares to regulate the wind speeds and thermal discomfort in the pedestrian-height-level atmosphere.
2. In northern temperate regions, the seasonal characteristics reflect cold conditions in winter and hot conditions in summer. Trees can effectively reduce the radiation temperature and thus regulate the temperature by affecting solar radiation penetration and changing the thermal environment under trees through the shading ability of the canopy. In relative outdoor spaces, the thermal environment can be improved by transplanting tall deciduous trees along the main walking axis of each functional area. The tall canopy provided by these trees can ensure stable shade in summer to improve the thermal environment by providing shading and cooling functions in summer, while in winter when the leaves fall, these trees do not affect the solar radiation to which the space is exposed.
3. With limited building coverage, it is crucial to ensure that building shadows can cover more space in summer while ensuring that sufficient outdoor space directly exposed to sunlight in winter. Changing the orientation of the buildings to control the angles between the buildings and the direct light could influence the building shadows, thus making full use of this characteristic. This would require calculating the relationships among the solar altitude, azimuth, and building orientation. By controlling the building shadows under the guarantee of satisfying the sunshine accessibility of indoor spaces, the outdoor space thermal comfort could be improved in a targeted way.

## 5. Conclusion

In this study, outdoor thermal comfort was evaluated by identifying the spatial morphology of the built environment of the Qingdao Univer-

sity of Technology campus and performing on-site measured and validated ENVI-met numerical simulations. The findings explicitly proved the need for the use of heat-mitigation techniques to cool these spaces and increase their usability. By analyzing the impacts of spatial morphology indices on the outdoor comfort of the university campus, the spatial morphology of the campus significantly impacts the outdoor thermal environment of the campus, in turn elucidating an optimization strategy for the spatial planning and design of the university campus.

- ENVI-met was found to be effective in predicting the university campus microclimate environment, with correlation coefficients greater than 0.85 and root mean squared errors (RMSE) ranging from 0.55 to 1.91.
- Comparing the B-B' (north–south) axis with the PET values on the A-A' (east–west) axis at 09:00, 12:00, 15:00, and 18:00 corresponding to the subjective thermal sensation percentage results showed that the subjective thermal sensation on both axes was strongest at 12:00 noon and weakest at 18:00. When the results were compared, both the mean PET and the proportion of subjective thermal sensation showed that the B-B' (north–south) axis was more comfortable than the A-A' (east–west) axis.
- SVF has a strong correlation with MRT and PET, according to the R<sup>2</sup> of the fit values at 09:00, 12:00, 15:00, and 18:00. At 9:00, 12:00, and 15:00, the SVF has a strong positive effect on MRT and PET. In contrast, the SVF has a strong negative correlation with MRT and PET at 18:00.
- According to the regression model results for four time periods (09:00, 12:00, 15:00, and 18:00), among the spatial morphological indicators, BD has the most significant influence on PET. This demonstrates that adjusting BD is a key step in improving the outdoor thermal environment.

## Funding

Not applicable.

## Data availability statement

Not applicable.

## Declaration of Competing Interest

The authors declare that they have no known competing financial interests or personal relationships that could have appeared to influence the work reported in this paper.

## CRediT authorship contribution statement

**Yansu Qi:** Conceptualization, Methodology, Writing – original draft. **Lan Chen:** Data curation, Software. **Jiuzhe Xu:** Visualization, Investigation. **Chao Liu:** Writing – review & editing. **Weijun Gao:** Supervision. **Sheng Miao:** Resources, Validation.

## Acknowledgments

Not applicable.

## References

- [1] P.W. Stark Da Silva, D. Duarte, S. Pauleit, The Role of the Design of Public Squares and Vegetation Composition on Human Thermal Comfort in Different Seasons a Quantitative Assessment, *Land* 12 (2023) 427.
- [2] C.K.C. Lam, J. Weng, K. Liu, J. Hang, The effects of shading devices on outdoor thermal and visual comfort in Southern China during summer, *Build. Environ.* 228 (2023) 109743.
- [3] Y. Su, Q. Zhao, N. Zhou, Improvement strategies for thermal comfort of a city block based on PET Simulation—A case study of Dalian, a cold-region city in China, *Energ. Build.* 261 (2022) 111557.
- [4] N. Gaber, A. Ibrahim, A.B. Rashad, E. Wahba, Z. El-Sayad, A.F. Bakr, Improving pedestrian micro-climate in urban canyons: City Center of Alexandria, Egypt, *Urban Climate* 34 (2020) 100670.
- [5] H. Wang, L. Liu, Experimental investigation about effect of emotion state on people's thermal comfort, *Energ. Build.* 211 (2020) 109789.
- [6] J. Li, N. Liu, The perception, optimization strategies and prospects of outdoor thermal comfort in China: A review, *Build. Environ.* 170 (2020) 106614.
- [7] D. Zhao, Y. Liu, G. Zeng, X. Wang, S. Miao, W. Gao, A Knowledge-Based Human-Computer Interaction System for the Building Design Evaluation Using Artificial Neural Network, *Hum.-Cent. Comput. Inf.* 13 (2023) 2.
- [8] E. Jamei, P. Rajagopalan, Urban development and pedestrian thermal comfort in Melbourne, *Sol. Energy* 144 (2017) 681–698.
- [9] W.T.L. Chow, S.N.A.B. Akbar, S.L. Heng, M. Roth, Assessment of measured and perceived microclimates within a tropical urban forest, *Urban For. Urban Green.* 16 (2016) 62–75.
- [10] P. Cui, J. Jiang, J. Zhang, L. Wang, Effect of street design on UHI and energy consumption based on vegetation and street aspect ratio: Taking Harbin as an example, *Sustain. Cities Soc.* 92 (2023) 104484.
- [11] C. Vasilikou, M. Nikolopoulou, Outdoor thermal comfort for pedestrians in movement: thermal walks in complex urban morphology, *Int. J. Biometeorol.* 64 (2020) 277–291.
- [12] M.W. Yahia, E. Johansson, Evaluating the behaviour of different thermal indices by investigating various outdoor urban environments in the hot dry city of Damascus, Syria, *Int. J. Biometeorol.* 57 (2013) 615–630.
- [13] D. Pearlmutter, P. Berliner, E. Shaviv, Integrated modeling of pedestrian energy exchange and thermal comfort in urban street canyons, *Build. Environ.* 42 (2007) 2396–2409.
- [14] J. Mi, B. Hong, T. Zhang, B. Huang, J. Niu, Outdoor thermal benchmarks and their application to climate-responsive designs of residential open spaces in a cold region of China, *Build. Environ.* 169 (2020) 106592.
- [15] Q.S.D.J. Zhao, Impact of Tree Locations and Arrangements on Outdoor Microclimates and Human Thermal Comfort in an Urban Residential Environment, *Urban For. Urban Green.* (2018).
- [16] A. Hami, B. Abdi, D. Zarehagi, S.B. Maulan, Assessing the thermal comfort effects of green spaces: A systematic review of methods, parameters, and plants' attributes, *Sustain. Cities Soc.* 49 (2019) 101634.
- [17] P. Marrone, F. Orsini, F. Asdrubali, C. Guattari, Environmental performance of universities: Proposal for implementing campus urban morphology as an evaluation parameter in Green Metric, *Sustain. Cities Soc.* 42 (2018) 226–239.
- [18] R.M.A. Mahmoud, A.S.H. Abdallah, Assessment of outdoor shading strategies to improve outdoor thermal comfort in school courtyards in hot and arid climates, *Sustain. Cities Soc.* 86 (2022) 104147.
- [19] D. Elgheznawy, S. Eltarably, The impact of sun sail-shading strategy on the thermal comfort in school courtyards, *Build. Environ.* 202 (2021) 108046.
- [20] A. Ghaffarianhoseini, U. Berardi, A. Ghaffarianhoseini, K. Al-Obaidi, Analyzing the thermal comfort conditions of outdoor spaces in a university campus in Kuala Lumpur, Malaysia, *Sci. Total Environ.* 666 (2019) 1327–1345.
- [21] Z. Yu, S. Chen, N.H. Wong, Temporal variation in the impact of urban morphology on outdoor air temperature in the tropics: A campus case study, *Build. Environ.* 181 (2020) 107132.
- [22] S.A. Zaki, N.E. Othman, S.W. Syahidah, F. Yakub, F. Muhammad-Sukki, J.A. Ardi-la-Rey, et al., Effects of Urban Morphology on Microclimate Parameters in an Urban University Campus, *Sustainability-Basel* 12 (2020) 2962.
- [23] H. Zhong, M. Guo, Y. Wang, Z. Wang, Quantify the magnitude and energy impact of overcooling in a sub-tropical campus building, *Build. Environ.* 231 (2023) 110033.
- [24] N. Mohammadzadeh, A. Karimi, R.D. Brown, The influence of outdoor thermal comfort on acoustic comfort of urban parks based on plant communities, *Build. Environ.* 228 (2023) 109884.
- [25] I. Kousis, A.L. Pisello, For the mitigation of urban heat island and urban noise island: two simultaneous sides of urban discomfort, *Environ. Res. Lett.* 15 (2020) 103004.
- [26] E.L. Krüger, D. Pearlmutter, The effect of urban evaporation on building energy demand in an arid environment, *Energ. Build.* 40 (2008) 2090–2098.
- [27] M. Park, A. Hagishima, J. Tanimoto, K. Narita, Effect of urban vegetation on outdoor thermal environment: Field measurement at a scale model site, *Build. Environ.* 56 (2012) 38–46.
- [28] G. Thomas, J. Thomas, G.M. Mathews, S.P. Alexander, J. Jose, Assessment of the potential of green wall on modification of local urban microclimate in humid tropical climate using ENVI-met model, *Ecol. Eng.* 187 (2023) 106868.
- [29] A. Alyakoob, S. Hartono, T. Johnson, A. Middel, Estimating cooling loads of Arizona State University buildings using microclimate data and machine learning, *J. Build. Eng.* 64 (2023) 105705.
- [30] M.W. Yahia, E. Johansson, Influence of urban planning regulations on the microclimate in a hot dry climate: The example of Damascus, Syria, *J. Hous. Built Environ.* 28 (2013) 51–65.
- [31] L. Chen, E. Ng, Outdoor thermal comfort and outdoor activities: A review of research in the past decade, *Cities* 29 (2012) 118–125.
- [32] F. Ali-Toudert, H. Mayer, Numerical study on the effects of aspect ratio and orientation of an urban street canyon on outdoor thermal comfort in hot and dry climate, *Build. Environ.* 41 (2006) 94–108.
- [33] F.A. Toudert, Dependence of Outdoor Thermal Comfort on Street Design in Hot and Dry Climate, University of Freiburg, 2005.
- [34] M.W. Yahia, E. Johansson, S. Thorsson, F. Lindberg, M.I. Rasmussen, Effect of urban design on microclimate and thermal comfort outdoors in warm-humid Dar es Salaam, Tanzania, *Int. J. Biometeorol.* 62 (2018) 373–385.
- [35] E. Fiorillo, L. Brilli, F. Carotenuto, L. Cremonini, B. Gioli, T. Giordano, et al., Diurnal Outdoor Thermal Comfort Mapping through Envi-Met Simulations, Remotely Sensed and In Situ Measurements, *Atmosphere-Basel*. 14 (2023) 641.
- [36] Z. Ren, Y. Fu, Y. Dong, P. Zhang, X. He, Rapid urbanization and climate change significantly contribute to worsening urban human thermal comfort: A national 183-city, 26-year study in China, *Urban Climate* 43 (2022) 101154.
- [37] K. Xin, J. Zhao, T. Wang, W. Gao, Supporting Design to Develop Rural Revitalization through Investigating Village Microclimate Environments: A Case Study of Typical Villages in Northwest China, *Int. J. Env. Res. Publ. He.* 19 (2022) 8310.
- [38] H. Yan, F. Wu, L. Dong, Influence of a large urban park on the local urban thermal environment, *Sci. Total Environ.* 622–623 (2018) 882–891.
- [39] Z. Yu, S. Chen, N.H. Wong, M. Ignatius, J. Deng, Y. He, et al., Dependence between urban morphology and outdoor air temperature: A tropical campus study using random forests algorithm, *Sustain. Cities Soc.* 61 (2020) 102200.
- [40] L. Chapman, J.E. Thornes, A.V. Bradley, Rapid determination of canyon geometry parameters for use in surface radiation budgets, *Theor. Appl. Climatol.* 69 (2001) 81–89.
- [41] C. Ketterer, A. Matzarakis, Human-biometeorological assessment of heat stress reduction by replanning measures in Stuttgart, Germany, *Landscape Urban Plan* 122 (2014) 78–88.
- [42] Y. Yang, D. Zhou, W. Gao, Z. Zhang, W. Chen, W. Peng, Simulation on the impacts of the street tree pattern on built summer thermal comfort in cold region of China, *Sustain. Cities Soc.* 37 (2018) 563–580.
- [43] D. Lai, D. Guo, Y. Hou, C. Lin, Q. Chen, Studies of outdoor thermal comfort in northern China, *Build. Environ.* 77 (2014) 110–118.
- [44] D.H.S. Duarte, P. Shinzato, C.D.S. Gusson, C.A. Alves, The impact of vegetation on urban microclimate to counterbalance built density in a subtropical changing climate, *Urban Climate* 14 (2015) 224–239.
- [45] X. He, W. Gao, R. Wang, Impact of urban morphology on the microclimate around elementary schools: A case study from Japan, *Build. Environ.* 206 (2021) 108383.
- [46] B.C. Hedquist, A.J. Brazel, Seasonal variability of temperatures and outdoor human comfort in Phoenix, Arizona, USA, *Build. Environ.* 72 (2014) 377–388.
- [47] M. Kolokotroni, Cool materials in the urban built environment to mitigate heat islands: potential consequences for building ventilation, (2017).
- [48] H. Lee, H. Mayer, L. Chen, Contribution of trees and grasslands to the mitigation of human heat stress in a residential district of Freiburg, Southwest Germany, *Landscape Urban Plan* 148 (2016) 37–50.
- [49] T.E. Morakinyo, K.K. Lau, C. Ren, E. Ng, Performance of Hong Kong's common trees species for outdoor temperature regulation, thermal comfort and energy saving, *Build. Environ.* 137 (2018) 157–170.
- [50] M.F. Shahidan, P.J. Jones, J. Gwilliam, E. Salleh, An evaluation of outdoor and building environment cooling achieved through combination modification of trees with ground materials, *Build. Environ.* 58 (2012) 245–257.
- [51] S. Sun, X. Xu, Z. Lao, W. Liu, Z. Li, E. Higuera García, et al., Evaluating the impact of urban green space and landscape design parameters on thermal comfort in hot summer by numerical simulation, *Build. Environ.* 123 (2017) 277–288.
- [52] Z. Tan, K.K. Lau, E. Ng, Urban tree design approaches for mitigating daytime urban heat island effects in a high-density urban environment, *Energ. Build.* 114 (2016) 265–274.
- [53] S. Tsoka, A. Tsikaloudaki, T. Theodosiou, Analyzing the ENVI-met microclimate model's performance and assessing cool materials and urban vegetation applications—a review, *Sustain. Cities Soc.* 43 (2018) 55–76.
- [54] Y. Wang, J. Zacharias, Landscape modification for ambient environmental improvement in central business districts – A case from Beijing, *Urban For. Urban Gree.* 14 (2015) 8–18.
- [55] X. Yang, L. Zhao, M. Bruse, Q. Meng, Evaluation of a microclimate model for predicting the thermal behavior of different ground surfaces, *Build. Environ.* 60 (2013) 93–104.
- [56] E.L. Krüger, F.O. Minella, F. Rasia, Impact of urban geometry on outdoor thermal comfort and air quality from field measurements in Curitiba, Brazil, *Build. Environ.* 46 (2011) 621–634.
- [57] E. Krüger, B. Givoni, Outdoor measurements and temperature comparisons of seven monitoring stations: Preliminary studies in Curitiba, Brazil, *Build. Environ.* 42 (2007) 1685–1698.
- [58] N. Nasrollahi, Y. Namazi, M. Taleghani, The effect of urban shading and canyon geometry on outdoor thermal comfort in hot climates: A case study of Ahvaz, Iran, *Sustain. Cities Soc.* 65 (2021) 102638.

- [59] Y. Xia, N. Yabuki, T. Fukuda, Sky view factor estimation from street view images based on semantic segmentation, *Urban Climate* 40 (2021) 100999.
- [60] M.M. Baruti, E. Johansson, M.W. Yahia, Urbanites' outdoor thermal comfort in the informal urban fabric of warm-humid Dar es Salaam, Tanzania, *Sustain. Cities Soc.* 62 (2020) 102380.
- [61] J. Xue, X. Hu, S.N. Sani, Y. Wu, X. Li, L. Chai, et al., Outdoor Thermal Comfort at a University Campus: Studies from Personal and Long-Term Thermal History Perspectives, *Sustainability-Basel* 12 (2020) 9284.
- [62] J. Xue, W. Liu, K. Liu, Influence of Thermal Environment on Attendance and Adaptive Behaviors in Outdoor Spaces: A Study in a Cold-Climate University Campus, *Int. J. Env. Res. Pub. He* 18 (2021) 6139.
- [63] C. Sun, W. Lian, L. Liu, Q. Dong, Y. Han, The impact of street geometry on outdoor thermal comfort within three different urban forms in severe cold region of China, *Build. Environ.* 222 (2022) 109342.
- [64] X. Deng, W. Nie, X. Li, J. Wu, Z. Yin, J. Han, et al., Influence of built environment on outdoor thermal comfort: A comparative study of new and old urban blocks in Guangzhou, *Build. Environ.* 234 (2023) 110133.
- [65] Y. Gao, J. Zhao, L. Han, Exploring the spatial heterogeneity of urban heat island effect and its relationship to block morphology with the geographically weighted regression model, *Sustain. Cities Soc.* 76 (2022) 103431.
- [66] J. Zhang, Z. Li, D. Hu, Effects of urban morphology on thermal comfort at the micro-scale, *Sustain. Cities Soc.* 86 (2022) 104150.